CHAPTER 5

LOCAL BUBBLE SIZE DISTRIBUTION

A one-dimensional population balance model for determining local bubble distributions in bubble column reactors is proposed in this chapter. This is also an example of using the turbulent coalescence and breakup rate models developed in Chapter 3. Bubble coalescence due to buoyancy is also considered and discussed.

The predicted results by this model for the air-water system in a tall column show that the bubble size distributions above the entrance region (H > 30 cm above the gas distributor) are stable and independent of the size distribution at the distributor. They show good agreement with those measured by the five-point conductivity probe technique, especially for the cases at high superficial gas velocities.

5.1 Introduction

As discussed before, the bubble distributions are of the most basic characteristics of bubble column reactors. The bubble properties such as size and concentration are decisive factors affecting the hydrodynamics and transport properties in the column, and determine averaged properties such as interfacial area or Sauter mean diameter; values which are often required in engineering problems.

However, not all bubbles have the same size or the same concentration. A bubble can vary in size due to changes in local temperature and pressure, and can disappear due to coalescence or breakup. Thus, there are distributions of bubble size and bubble concentration, which are functions of the coordinate. In order to obtain bubble size distributions, it is necessary to describe the bubble-bubble interactions such as coalescence and breakage. The most important deterministic model for doing this is based on the population balance concept. A significant advantage of the population balance is to provide a path to include the details of the breakage and coalescence processes according to the physical properties and operating conditions. It has been used for many processes including crystallization, polymerization and fermentation.

The population balance concept or technique is very similar to other conservation ideas such as mass, heat and momentum. The technique itself may even be even simpler, since it considers the balance of countable entities such as bubbles, drops or crystals. The difficulty in the population balance technique is how to obtain models describing the birth and death processes for the countable entities in question.

Early, the concept of a population balance was used in describing processes such as crystallization, polymerization and fermentation in stirred vessels, where growth and shrinkage of particles are dominant (Randolph and Larson, 1962; Behnken *et al.*, 1963; Fredrickson and Tsuchiya, 1963). It was later developed for determining the drop size distributions in liquid-liquid dispersions (Valentas and Amundson, 1966; Valentas *et al.* 1966; Coulaloglou and Tavlarides, 1977; Narsimhan *et al.*, 1979; Chatzi *et al.*, 1989; Chatzi and Kiparissides, 1992, Nambiar *et al.*, 1992), as mentioned in Chapter 3. In these cases, drop coalescence and breakup processes exist simultaneously. However, the modeling work is relatively simple in these systems, because drop size distributions, as well as drop coalescence and breakage rates, can be considered to be spatially homogeneous in a stirred tank.

The situation in bubble columns is more complex since bubble size distributions usually depend also on the coordinates. Hence, the coalescence and breakup rates vary spatially, too. This may be the reason why little work has been done for

predicting bubble size distributions in bubble columns. Another reason may be that it is more difficult to establish models for bubble coalescence and breakup rates.

Mihail and Straja (1986) used the population balance technique to analyze the one-dimensional bubble size distribution in a bubble column. However, as mentioned in Chapter 3, they had to tune four parameters in their coalescence and breakup rate models. Lee *et al.* (1987b) used a population balance method for non-coalescing systems, where the bubble escape frequency or bubble rising velocity was assumed to be constant for all sizes of bubbles. Recently, Hesketh *et al.* (1991b) studied bubble breakup in pipeline flows at very low gas fraction using a population balance method and specially assumed that the breakage frequency and efficiency were independent of bubble size.

In this chapter, the local bubble size distributions are predicted using a one-dimensional population balance model together with the rate models of bubble coalescence and breakup developed in Chapter 3.

5.2 Population Balance Model

5.2.1 Equations of balance

A general population balance equation for countable entities was developed by Randolph (1964). For bubbles of volume v_i or diameter d_i (i = 1, 2, ..., N), the number density is $n_i(v_i,X,t)$, that is a function of size v_i or d_i, spatial vector X and time t. According to Randolph (1964), the population equation can be expressed as

$$\frac{\partial n_i}{\partial t} + \nabla\cdot\vec{u}n_i = BC + BB - DC - DB \tag{5.1}$$

where $\vec{u}$ is the average velocity vector of dispersion, and BC, BB, DC and DB

are the bubble number birth and death rates per unit dispersion volume for bubbles of size v_i or d_i at time t due to coalescence and breakage respectively. These are then functions of bubble size v_i, bubble density n_i, spatial vector X and time t.

For simplicity and convenience, the dispersion in a bubble column can be considered as a series of (one or more) well-mixed cells. For each well-mixed cell, the bubble number density can be considered to be uniform in the cell. For a well-mixed cell with constant volume ΔV_R, the population balance equation can be derived from Equation (5.1) (Randolph, 1964) as follows.

$$\frac{\partial n_i}{\partial t} = BC + BB - DC - DB + \frac{(Qn_i)_{in}}{\Delta V_R} - \frac{(Qn_i)_{out}}{\Delta V_R} \tag{5.2}$$

where Q is the volumetric flow rate of dispersion. For this equation, the assumption that bubble number densities are homogeneous in the dispersion has been used. Obviously, Equation (5.2) can also be obtained directly from the number balance of bubble i in a well-mixed vessel with volume ΔV_R.

In this work, only the change of bubble number density in the axial direction at steady state is considered. Hence, ΔV_R can be set equal to the volume of a column section or cell, $A_c \Delta H$, as shown in Figure 5.1. If ΔH is small enough, the bubble size change due to pressure (for simplification, only isothermal systems are considered in this work) in the cell is negligible. Thereby the volumetric flow rates can be considered to be constant inside the cell volume and equal $(Q)_{in}$.

For the one-dimensional model, $Q = Q_G + Q_L$. Therefore, from Equation (5.2), the population balance equation at steady state can be expressed by

$$\frac{(u_G + u_L)_{in}}{\Delta H}(n_i - n_{i,in}) = BC + BB - DC - DB \tag{5.3}$$

where $u_G = Q_G/A_c$ and $u_L = Q_L/A_c$ have been used. It should be noted that BC,

BB, *DC* and *DB* for bubbles of size v_i are now only functions of v_i and n_i at steady state. They can be expressed by the coalescence and breakup rate models developed in Chapter 3.

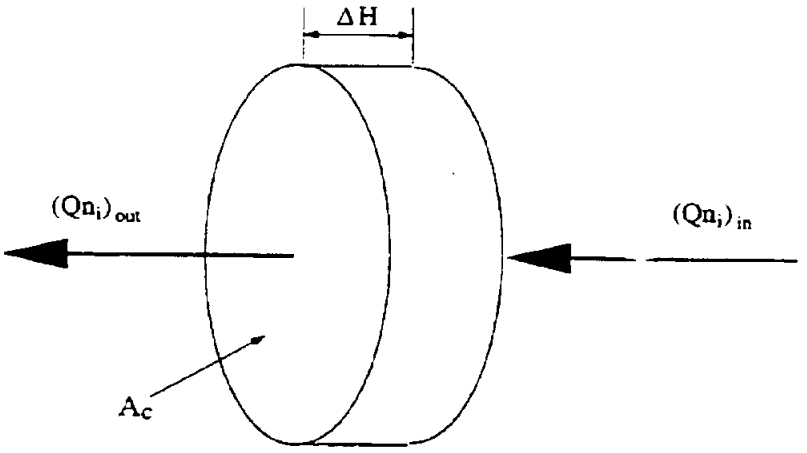

Figure 5.1 Sketch of the bubble column cell for population balance.

The birth of bubbles of size v_i due to coalescence is from the coalescence between all bubbles of size smaller than v_i. Hence, the birth rate for bubbles of size v_i, *BC*, can be obtained by summing all coalescence events that form a bubble of size v_i. This gives

$$BC = \sum_{v_j = v_{min}}^{v_i/2} \Omega_C(v_j : v_i - v_j) \tag{5.4}$$

where v_{min} is the minimum bubble size and depends on the minimum eddy size

in a system. It was taken as zero by some investigators like Lee *et al.* (1987). Equation (5.4) implies that bubbles of size v_j coalesce with bubbles of size (v_i-v_j) to form bubbles of size v_i. The upper limit of the sum stems from the symmetry consideration, or, avoids counting the coalescence between the same pair of bubble sizes twice.

Similarly, the death of bubbles of size v_i due to coalescence is by coalescence between themselves and other bubbles. Hence, the bubble death rate for bubbles of size v_i, DC, can be calculated by

$$DC = \sum_{v_j=v_{min}}^{v_{max}-v_i} \Omega_C(v_j:v_i) \tag{5.5}$$

where v_{max} is the maximum bubble size in the system. The upper limit indicates that the bubble volume formed by coalescence will not exceed v_{max}.

The birth of bubbles of size v_i due to breakage is from the breakup of all bubbles larger than v_i ($v_j \geq v_i$). The breakage birth rate, BB, can be obtained by summing all the breakup events that form the bubbles of size v_i:

$$BB = \sum_{v_j=v_i}^{v_{max}} \Omega_B(v_j:v_i) \tag{5.6}$$

The death of bubbles of volume v_i due to breakup is by the breakage of themselves, thus

$$DB = \Omega_B(v_i) \tag{5.7}$$

Hence, Equation (5.3) can be rewritten as

$$\frac{(u_G/\varepsilon_G)_{in}}{\Delta H}(n_i - n_{i,in}) = \sum_{v_j=v_{min}}^{v_i/2} \Omega_C(v_j:v_i-v_j) - \sum_{v_j=v_{min}}^{v_{max}-v_i} \Omega_C(v_j:v_i) + \sum_{v_j=v_i}^{v_{max}} \Omega_B(v_j:v_i) - \Omega_B(v_i) \tag{5.8}$$

Since Ω_C and Ω_B are functions of n_i and/or n_j (see Chapter 3), Equation (5.8) is a non-linear system of N equations (for N bubble size classes).

When solving Equation (5.8) for each column cell, the number density, n_i (i = 1, 2, ...), and the flow rate, u_G+u_L, at the inlet of the column cell are known to equal those at the outlet of the previous cell, since the cells are continuous in series. However, for the first column cell counted from the gas distributor, the inlet conditions need to be estimated or given, according to the geometry of the gas distributor and the operation conditions. This will be discussed later.

When the bubble density for a column section or cell, n_i, is obtained, the average gas holdup in the cell and at the outlet can be calculated by

$$\varepsilon_G = \sum_{v_i=v_{min}}^{v_{max}} n_i v_i \tag{5.9}$$

5.2.2 Viscous and buoyancy coalescence

In bubble columns, collisions or coalescence may occur due to a variety of mechanisms such as turbulence, shear stress and buoyancy (Prince and Blanch, 1990). Turbulent collisions result from the random motion of bubbles due to turbulence. The second collision mechanism is termed "viscous collisions" or "shear collisions", in which bubbles in a region of relatively high liquid velocity

may collide with bubbles in the slower section of the velocity field, since there exists a velocity gradient in the liquid (especially with high liquid circulation). The third is due to the difference in rise velocities between bubbles of different sizes and is called "buoyancy collisions". The turbulent collisions and coalescence have been discussed and modeled in Chapter 3. The other mechanisms for collision and coalescence are discussed in the following.

For viscous collisions, the collision frequency can, as for the turbulent collisions, be determined by Equation (3.5). However, the approach or collision velocity is different and can be obtained according an equation developed by Friedlander (1977). This gives

$$u_{ij} = \frac{16}{3\pi}\left(d_i + d_j\right)\left|\frac{du_l}{dr}\right| \tag{5.10}$$

Since only one-dimensional changes are considered in this population balance model and the turbulent collision mechanism is thought to dominate, the collisions or coalescence due to the viscous mechanism is disregarded.

For the collisions due to buoyancy, the approach velocity between two bubbles can also obtained from the work of Friedlander (1977)

$$u_{ij} = \left|u_{bi} - u_{bj}\right| \tag{5.11}$$

Where u_{bi} and u_{bj} are the bubble rise velocities in liquid and can be considered to equal the terminal velocities (Prince and Blanch, 1990).

Knowing the approach velocity due to buoyancy, the corresponding collision frequency can be determined by Equation (3.5). Assuming that Equation (3.9) is also suitable for determining the coalescence efficiency for the buoyancy coalescence case, the buoyancy coalescence rate can be calculated using the same procedure as in Chapter 3. This assumption may be questionable since the coalescence time used to develop Equation (3.9) is based on turbulent mecha-

nism. Nevertheless, in the absence of more reasonable models, this is a method giving a first estimate for the coalescence rate due to buoyancy.

5.2.3 Energy dissipation rate

There are several methods for estimating the energy dissipation rate per unit liquid mass, ε, used in the expressions for coalescence and breakup rates (see Chapter 3). Prince and Blanch (1990) proposed an equation for estimating the average energy dissipation rate over the whole column, based on an expression for the power input to gas sparged vessels developed by Bhavaraju *et al.* (1978). The dissipation rate can also be obtained by integrating the liquid velocity profile from a liquid circulation model (Geary and Rice, 1992).

Since the turbulence in bubble columns is usually induced by bubbles, the energy dissipation rate can simply be estimated from the drag forces and the slip velocities. In other words, the energy dissipation rate for a bubble is the product of the drag force and the slip velocity between the bubble and the liquid (Jin and Kim, 1990). At steady state, the drag force equals the buoyancy force so that the energy dissipation rate of a bubble can be expressed by $\Delta\rho g v_i u_{s,i}$. Then the energy dissipation rate per unit dispersion volume is

$$\varepsilon_v = \Delta\rho g \sum n_i v_i u_{s,i} = \Delta\rho g u_G \tag{5.12}$$

Thus, the energy dissipation rate per unit liquid mass can be estimated by

$$\varepsilon = \frac{\varepsilon_v}{\rho_L(1-\varepsilon_G)} = \frac{\Delta\rho g u_G}{\rho_L(1-\varepsilon_G)} \tag{5.13}$$

It can be noted that the real superficial gas velocity varies with the axial position in a column due to the pressure drop and the gas volume expansion.

5.2.4 Boundary conditions

As mentioned above, the bubble sizes, number densities and gas holdup close to or at the gas distributor should be known before the population balance model can be solved.

Unfortunately, these boundary conditions are usually difficult to predict, due to the complexity of the liquid circulation near the gas distributor. However, the bubble sizes formed by the gas distributor can be estimated from theoretical or semi-theoretical correlations (Ramakrishnan *et al*, 1969; Marmur and Rubin, 1976; Blass, 1990; Geary and Rice, 1991). At a low gas velocity ($u_h^2\rho_G d_h/\sigma < 2$, where u_h is the hole gas velocity and d_h is the hole diameter), the formed bubble sizes are nearly uniform (Blass, 1990). At high gas velocity ($u_h^2\rho_G d_h/\sigma \geq 2$), two bubble sizes may simultaneously be formed (primary and secondary bubble sizes).

In order to estimate the boundary conditions at the gas distributor, a uniform distributed bubble size, d_{inlet}, is assumed. Furthermore, it is supposed that there are only the bubbles formed by the distributor in the thin layer of height d_{inlet} close to the distributor. The average gas holdup in the thin layer is therefore estimated by

$$\varepsilon_{G,inlet} - \varepsilon_{G,\min} = \frac{N_h(\pi/6)d_{inlet}^3}{A_c d_{inlet}} = \frac{2N_h}{3}\left(\frac{d_{inlet}}{D_c}\right)^2 \qquad (5.14)$$

where N_h is the hole number for gas flow on the gas distributor. In this equation, the real void fraction in the thin layer, $\varepsilon_{G,inlet}$, should be larger than $\varepsilon_{G,min}$, since there must exist other bubbles besides the distributed bubbles, due to the effect of liquid circulation. Hence, if there are large discrepancies between the values estimated from this equation and the experimental results near to the gas distributor, the estimated values should be given up and more reasonable boundary gas holdups need to be assumed.

Knowing the gas holdup close to the gas distributor, when the bubble sizes in the layer close to the distributor are considered to be uniform, the corresponding bubble number density, n_{inlet}, can then be calculated by

$$n_{inlet} = \frac{\varepsilon_{G,inlet}}{(\pi/6)d_{inlet}^3} \tag{5.15}$$

5.3 Results and Discussion

All calculations in this work were done for the air-water system in the bubble column described in Chapter 2, using a personal computer. According to the experimental measurements by the five-point conductivity probe technique (see Chapter 2), the possible maximum bubble sizes were found to be about 20 mm. Hence, considering the computation time, 50 bubble size classes in the range of 0-20 mm were used in the calculations. There is no doubt that using more bubble size classes can enhance the computational accuracy, but it will also rapidly increase computation time. The height of a column cell (well-mixed) was set to be 2 cm.

Figure 5.2 and Figure 5.3 show the calculated bubble size distributions at various heights in the column for u_G = 17 cm/s, with considering the buoyancy coalescence. At this gas velocity, the gas flow in the holes of the gas distributor is in the "jet regime" ($u_h^2\rho_C d_h/\sigma \geq 2$). According to the results of Blass (1990), the bubble sizes formed by a perforated plate distributor with hole diameter 1 mm are in the range 5-9 mm. Lower values may be obtained from other correlations (*e.g.* Geary and Rice, 1991; Marmur and Rubin, 1976). Hence, the conditions d_{inlet} = 5 and 9 mm were used for testing. The gas holdup near the distributor was set to be 0.2 that is about 1–4 times as $\varepsilon_{G,min}$. The results were also compared to those measured by the five-point probe technique, as shown in the figures.

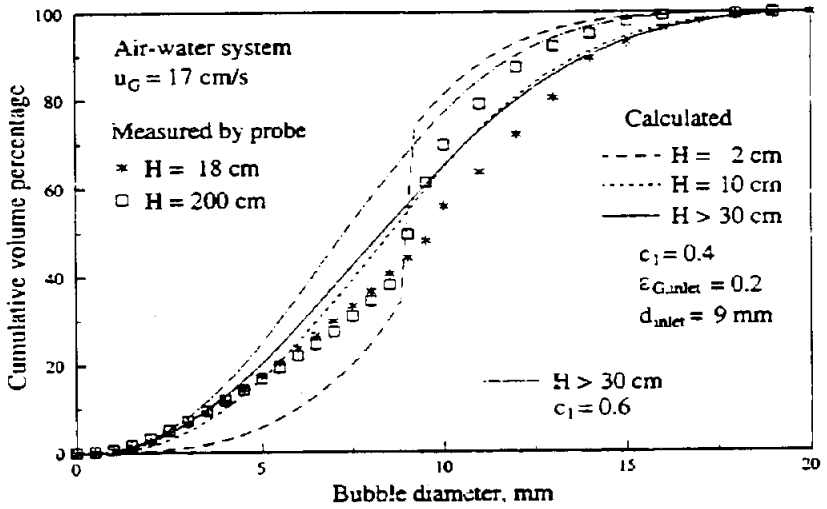

Figure 5.2 Calculated cumulative volume percentage at u_G = 17 cm/s using d_{inlet} = 5 mm, compared to the measured result.

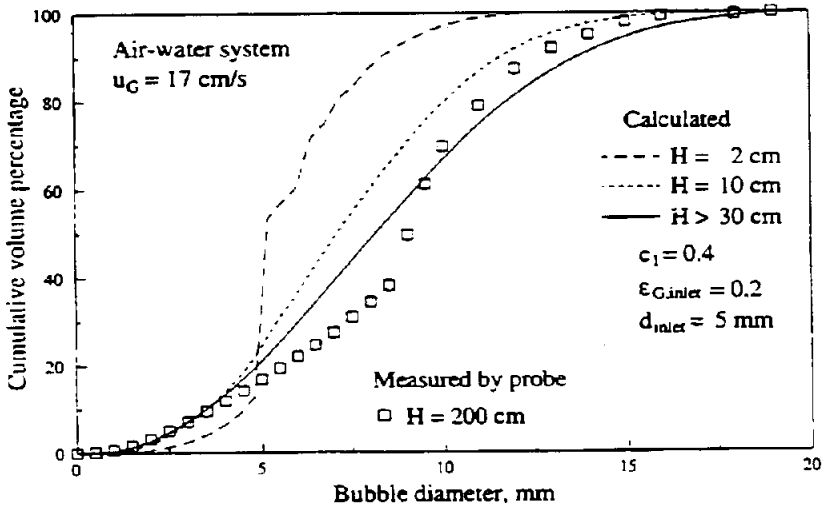

Figure 5.3 Calculated cumulative volume percentage at u_G = 17 cm/s using d_{inlet} = 7 mm, compared to the measured result.

From Figure 5.2 and Figure 5.3, it is seen that, at $H < 20$ cm, the bubble size distributions change fast due to the initial uniform bubbles coalescing into large bubbles and breaking into small bubbles. At $H = 20$-30 cm, the rates of coalescence and breakup become equal and the bubble size distributions, for both cases $d_{inlet} = 5$ mm and $d_{inlet} = 9$ mm, show little change with height. From $H > 30$ cm, the bubble size distributions have remains constant. The predicted stable bubble size distribution is identical for both cases and is in good agreement with the result obtained from the probe measurement at $H = 200$ cm.

Comparing Figure 5.2 and Figure 5.3, it is found that clear differences for the bubble size distributions for the two cases, $d_{inlet} = 5$ mm and $d_{inlet} = 9$ mm, only exist in the region $H < 30$ cm. At $H \geq 30$ cm, nearly no difference is found between the bubble size distributions (This can also be seen from Figure 5.4 showing the changes in calculated Sauter mean diameter). This indicates that the bubble size distributions in the air-water system are not sensitive to the inlet distribution of bubble sizes. In the other words, the type of gas distributors may have little effect on the bubble size distributions in such systems where there are strong coalescence and breakup tendencies. This conclusion agrees with that of Prince and Blanch (1990).

As seen from Figure 5.2, the predicted bubble size distributions close to the gas distributor are not representative of the real cases. This may be caused by the boundary condition, that is, the uniform bubble size distribution at the distributor may deviate significantly from reality. These discrepancies may be ignored for such systems where there are strong bubble coalescence and breakup tendencies in tall columns, since in these systems the bubble size distribution above the entrance region (about $H > 30$ cm) is nearly independent of the size distribution at the boundary. However, for short columns, low turbulence and low coalescing systems, better or more exact boundary conditions are needed.

From Figure 5.2, the effect of the constant, c_1, in the coalescence rate model (see Chapter 3) is also found. An increase in the value of c_1 (from 0.4 to 0.6) makes the coalescence efficiency and thereby the coalescence rate decrease. Thus, more bubbles with small sizes are obtained.

Figure 5.4 shows the changes in calculated Sauter mean diameter and the total bubble number density with the column height, for d_{inlet} = 5 mm and d_{inlet} = 9 mm respectively. It is found that the Sauter mean diameters are different and vary below a height of about 50 cm. Above this level, they become identical and slightly change from 6.6 mm to 7.2 mm (this change is caused by the decrease in pressure). This agrees well both with the result determined by the dynamic gas disengagement technique (see Figure 7.3) and that measured by the five-point conductivity probe technique (d_s = 7.2 mm). The total bubble densities are seen to be stable above a height of about 50-60 cm.

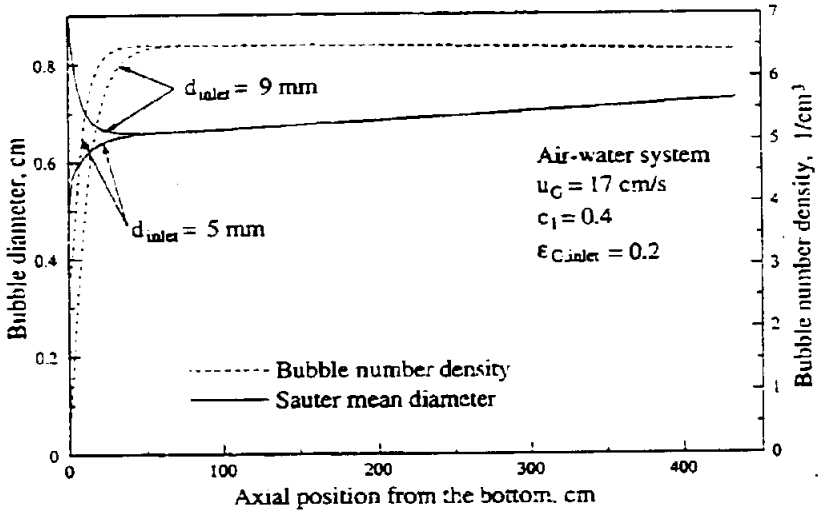

Figure 5.4 Changes of the Sauter mean bubble size and the total bubble number density with the column height.

The calculated bubble size distributions at u_G = 6 cm/s are also in good agreement with the measured results, as shown in Figure 5.5. However, the predicted volume fractions for small bubbles (about < 6-8 mm) are lower than the measured results. Similar variances can also be found in Figure 5.2 and Figure 5.3, and also from the work of Lee *et al.* (1987b) where bubble coalescence was disregarded. The discrepancies may mainly be caused by the coalescence rate

model used, since it has not been directly verified by experiments (Chapter 3).

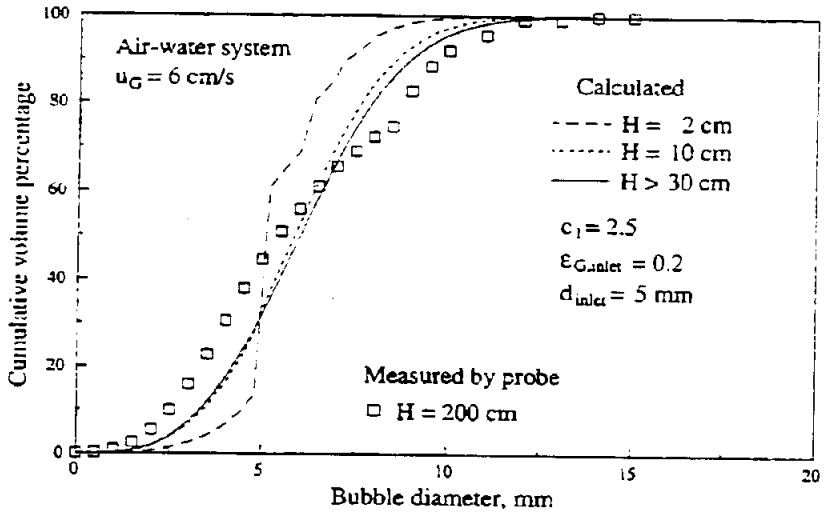

Figure 5.5 Calculated cumulative bubble volume percentage at u_G = 8 cm/s using d_{inlet} = 5 mm, comparing to the measured by the five-point probe.

In the coalescence rate model, the expression of coalescence efficiency, Equation (3.6), is in fact an empirical function. The relationship between the efficiency and the interaction and coalescence times may not be so simple, as discussed in Chapter 3. This can also be found from the value change of c_1, which has to be tuned to 2.5 for u_G = 6 cm/s in order to obtain a reasonable fit. This indicates that c_1 is a parameter depending on the superficial gas velocity or the flow regime. In this model, from Equation (5.13) it is seen that the superficial gas velocity affects the results through the energy dissipation rate, ε. This means that c_1 includes the effect of the energy dissipation rate. In addition, the coalescence time expression (Chesters, 1991) used in the coalescence rate model may not be completely correct for our system, since the former is derived from the fully-mobile interface assumption while a partial mobility is more probable for the air-tap water system.

Another reason for the discrepancies may be from the simplification in this population balance model. This model has ignored the radial and backward flows of the dispersion. In addition, it has assumed that the bubble number densities are homogeneous in the dispersion flow, Q, which may deviate from reality. For instance, for bubble i, the number flow rate into a control volume should be $Q_i n_i$ ($\Sigma Q_i = Q$), instead of $Q n_i$.

Nevertheless, this model does not give unreasonable results and seems to be better than the models found in the literature so far (*e.g.* Mihail and Straja, 1986; Lee *et al.*, 1987b). Especially this model has only one unknown parameter c_1, while the model of Lee *et al.* (1987) has two adjustable parameters (without consideration of bubble coalescence) and the model of Mihail and Straja (1986) has four parameters.

5.4 Conclusion

A one-dimensional population balance model for determining the bubble size distribution has been proposed. This model gives an example as to the use of the coalescence and breakup rate models developed in Chapter 3. The population balance model has only one unknown parameter, c_1, that is from the coalescence rate model. The predicted results above the entrance region for the air-water system in a tall bubble column by this population balance model seem to be in reasonable agreement with the measured results by the five-point conductivity probe technique.

The model shows that, for the air-water system, the bubble size distribution above the entrance region of the column is not sensitive to the inlet bubble size distribution at the gas distributor.

However, the predicted results have shown that c_1 in the coalescence rate model is a system and flow regime dependent parameter. This may indicate that the coalescence rate model needs to be further improved. Of course, effects of other

factors such as liquid viscosity, liquid density and inlet gas holdup (a boundary condition) may need to examine by this model in the future.

To improve the model further, the effects of liquid circulation and non-homogeneous distributed of bubble densities in dispersion should be included to the population balance model, and two-dimensional balance may also be needed.